

Developmental Cell

Small Ubiquitin-like modifier protein, SUMO enables plants to control growth independently of the phytohormone Gibberellic acid

--Manuscript Draft--

Manuscript Number:	DEVELOPMENTAL-CELL-D-12-00877R3
Full Title:	Small Ubiquitin-like modifier protein, SUMO enables plants to control growth independently of the phytohormone Gibberellic acid
Article Type:	Short Article
Keywords:	DELLAs plants growth SUMO Ubiquitin Hormone Gibberellic acid
Corresponding Author:	Ari Sadanandom University of Durham Durham, County Durham UNITED KINGDOM
First Author:	Lucio Conti, PhD
Order of Authors:	Lucio Conti, PhD Stuart Nelis, MSc cunjing zhang, PhD Ailidh Woodcock Ranjan Swarup, PhD Massimo Galbiati, PhD Chiara Tonelli, PhD Richard Napier Peter Hedden, PhD Malcolm Bennett, PhD Ari Sadanandom
Abstract:	<p>Plants survive adverse conditions by modulating their growth in response to changing environmental signals. Gibberellins (GA) play a key role in these adaptive responses by stimulating the degradation of growth repressing DELLA proteins. GA binding to its receptor GID1 enables association of GID1 with DELLAs. This leads to the ubiquitin-mediated proteasomal degradation of DELLAs and consequently growth promotion. We report that DELLA-dependent growth control can also be regulated independently of GA. We demonstrate that a proportion of DELLAs are conjugated to the Small Ubiquitin-like Modifier (SUMO) protein which increases during stress. We identify a SUMO interacting motif (SIM) in GID1 and demonstrate that SUMO-conjugated DELLA binds to this motif in a GA-independent manner. The consequent sequestration of GID1 by SUMO-conjugated DELLAs leads to an accumulation of non-SUMOylated DELLAs and subsequent beneficial growth restraint during stress. We conclude that plants have developed a non-GA mechanism to control growth during stress.</p>

Small Ubiquitin-like modifier protein, SUMO enables plants to control growth independently of the phytohormone gibberellin

Lucio Conti^{abc+}, Stuart Nelis^{a+}, Cunjin Zhang^a, Ailidh Woodcock^{a,f}, Ranjan Swarup^d, Massimo Galbiati^{bc}, Chiara Tonelli^{bc}, Richard Napier^f, Peter Hedden^e, Malcolm Bennett^d and Ari Sadanandom^{a*}

^aSchool of Biological and Biomedical Sciences, South Road, Durham University, DH1 3LE, UK

^bDepartment of Life Sciences, Università degli Studi di Milano, Via Celoria, 26 20133 Milano, Italy

^cFondazione Filarete Viale Ortles 22/4 20139 Milan, Italy

^dPlant Sciences Division, School of Biosciences, University of Nottingham, Sutton Bonington Campus, Loughborough, LE12 5RD, UK

^eRothamsted Research, West Common, Harpenden, Hertfordshire, AL5 2JQ, UK

^fSchool of Life Sciences University of Warwick, Gibbet Hill Road, Coventry, CV4 7ES, UK

+: Contributed equally to this work

*: corresponding author

SUMO controls DELLA accumulation independently of GA

SUMMARY

Plants survive adverse conditions by modulating their growth in response to changing environmental signals. Gibberellins (GAs) play a key role in these adaptive responses by stimulating the degradation of growth repressing DELLA proteins. GA binding to its receptor GID1 enables association of GID1 with DELLAs. This leads to the ubiquitin-mediated proteasomal degradation of DELLAs and consequently growth promotion. We report that DELLA-dependent growth control can also be regulated independently of GA. We demonstrate that a proportion of DELLAs are conjugated to the Small Ubiquitin-like Modifier (SUMO) protein, the extent of conjugation increasing during stress. We identify a SUMO interacting motif (SIM) in GID1 and demonstrate that SUMO-conjugated DELLA binds to this motif in a GA-independent manner. The consequent sequestration of GID1 by SUMO-conjugated DELLAs leads to an accumulation of non-SUMOylated DELLAs and subsequent beneficial growth restraint during stress. We conclude that plants have developed a GA-independent mechanism to control growth during stress.

HIGHLIGHTS

- A proportion of DELLAs are SUMOylated and this determines the overall DELLA levels independent of GA.
- During stress SUMOylated DELLA levels increase to elevate overall DELLA abundance.
- The GA receptor GID1, which is crucial for DELLA degradation, can also bind SUMOylated DELLA via its SUMO interacting (SIM) motif independent of GA.
- SUMO inhibits GID1 binding to non-SUMOylated DELLA and allows its accumulation and consequent growth restraint during stress.

INTRODUCTION

The sessile nature of plants dictates that growth must be integrated with changes in the natural environment. Current evidence indicates that a key strategy employed by plants to survive adverse conditions is to restrain growth via DELLA accumulation (Achard et al., 2006; 2008a; 2008b; Hou et al., 2010; Navarro et al., 2008). DELLA proteins are the central repressors of molecular pathways governed by the growth promoting phytohormone gibberellin (GA) (Ikeda et al., 2001; Peng et al., 1997; 1999; Silverstone et al., 1997). Recently it was shown that DELLA protein levels are critical for the coordination of plant development by light and GA (de Lucas et al., 2008; Feng et al., 2008). The integrative role of DELLAs is heavily reliant on the plant's ability to control DELLA protein levels, in turn mainly controlled through modulating the levels of GA. The current model for GA signalling describes how this hormone binds to its receptor GID1 so promoting association of GID1 with DELLA (Asako Shimada et al., 2008; Griffiths et al., 2006; Murase et al., 2008; Ueguchi-Tanaka et al., 2005; 2007; Willige et al., 2007) to trigger ubiquitin-mediated proteasomal degradation (Dill and T Sun, 2001; Fu et al., 2002; 2004; Itoh et al., 2002; McGinnis et al., 2003; Silverstone et al., 2001; Wang et al., 2009). Several other ubiquitin-like proteins have been described in plants including SUMO that can act to stabilize the proteins with which it is conjugated (Miura et al., 2009). SUMO proteases remove this protein tag to destabilize the de-conjugated protein (Lee et al., 2006). Here we demonstrate a role for SUMOylation in stabilising DELLA proteins under stress conditions. We provide evidence for a new molecular pathway for regulating plant growth that does not rely on GA levels.

RESULTS

Loss of *OTS* results in increased DELLA levels independently from GA

Arabidopsis mutant seedlings lacking the SUMO proteases OTS1 and OTS2 exhibit an enhanced inhibition of root growth when exposed to a 100 mM salt stress compared with wild type (Conti et al., 2008) (Figure 1A). Since DELLA have been shown to modulate root growth responses upon salt conditions (Achard et al., 2006), we addressed whether they contribute to the reduced growth phenotype of *ots1 ots2* in the presence of salt by creating an *ots1 ots2 rga* triple mutant, which lacks the RGA DELLA protein. Indeed loss of RGA function was sufficient to alleviate the reduced root growth phenotype of *ots1 ots2* double mutant on this permissive concentration of NaCl (Figure 1A, B). SUMO proteases participate in different developmental responses in *Arabidopsis* including flowering (Conti et al., 2008; Reeves et al., 2002). While *ots1 ots2* mutants are early flowering compared with type, *ots1 ots2 rga* triple mutants were even earlier flowering, suggesting that OTS and DELLA may also act separately (additively) in affecting the floral transition (Figure S1F). Further observations confirmed that *ots1 ots2* plants were affected in other GA-mediated processes including germination, mediated by DELLAs with more specialized functions (e.g. RGL2) (Lee et al., 2002; Tyler et al., 2004), (Figure S1A, B, C). Hence, the *ots1 ots2* mutant reveals a novel link between SUMOylation and DELLA-mediated growth regulation. To directly assess the impact of the *ots1 ots2* mutations on DELLA protein abundance, immunoblot experiments were performed. This revealed that endogenous levels of RGA and GAI DELLA proteins were more abundant in the *ots1 ots2* mutant plants compared to wild type (Figure 1C). Moreover, RGA accumulation was even more pronounced when *ots1 ots2* plants are grown on salt-

containing medium (Figure 1C). The current model for GA signalling dictates that regulation of the abundance of DELLA proteins is directly related to changes in levels of GA. However, we observed that there were no significant differences in GA levels between *ots1 ots2* mutant and wild type plants (Figure 1D). Nor did we find substantial differences in gene expression of *RGA*, *GAI* or well-established GA biosynthetic enzymes in the *ots1 ots2* mutant in the presence or absence of 100 mM NaCl (Figure S1D and E). Our data indicates that OTS1 and OTS2 have a separate additive effect along with GA on DELLA stability during salt stress. Since increased *DELLA* gene transcription or altered GA accumulation could not account for the increased DELLA protein accumulation observed in *ots1 ots2* mutants, we hypothesized that it could be caused by a novel GA-independent posttranslational mechanism.

SUMOylation is a novel peptide modification of DELLA

We next addressed whether SUMOylation of DELLA proteins could provide such a GA-independent mechanism for stabilising DELLAs. Taking advantage of a well-established transgenic line in which *RGA* is expressed as a functional GFP fusion under the endogenous *RGA* promoter (Silverstone et al., 2001) (*pRGA::GFP:RGA*) we immunopurified GFP:RGA protein under stringent conditions using GFP antibody-coated beads. GFP antibody detection revealed several forms of GFP:RGA in the immunoprecipitate migrating at higher molecular weight than the non-modified GFP:RGA protein. Arabidopsis SUMO1-specific antibodies indicated that these higher molecular weight forms of GFP:RGA were conjugated to SUMO1 (Figure 2A). To confirm that these SUMOylated GFP:RGA forms were targets for OTS1 SUMO protease

action we incubated the immunoprecipitate with purified OTS1 SUMO protease as well as a catalytically inactive form of OTS1 (OTS1^{C526S}). This treatment resulted in the dramatic reduction of the higher molecular weight, anti-SUMO1 cross-reacting bands only in the tubes containing wild-type OTS1, strongly indicating that OTS1 SUMO protease directly deSUMOylates DELLA proteins (Figure 2B, S2B). Further controls excluded the possibility that the SUMOylated forms of GFP:RGA could be derived from non-specific SUMOylation of GFP (Figure S2A). If SUMOylation represented an important regulatory mechanism for DELLA stability in plants, we would expect the site of conjugation to be highly conserved in DELLA sequences across all plant species. Using a bacterial SUMOylation system (Okada et al., 2009) we established that lysine 65 is the critical amino acid for SUMO attachment on RGA (Figure 2C). Strikingly, this SUMOylation site lysine residue is conserved across all DELLA proteins in Arabidopsis and other plant species including monocots (Figure 2D). Indeed we also demonstrated that the other major growth regulating DELLA protein, GAI is also SUMOylated *in vivo* and *in vitro* although this modification is more abundant upon salt stress (Figure 2E and S2F). This remarkable conservation of the SUMO site in DELLAs from divergent plant species is consistent with this mechanism playing a critical role in DELLA signalling.

SUMOylation-dependent DELLA accumulation

To gain more insight into the role of DELLA SUMOylation and its interplay with the non-SUMOylated DELLA, we analysed the pattern of accumulation of the SUMOylated RGA pool in conditions known to stimulate DELLA accumulation. We found that conditions that promote DELLA accumulation (high salinity) also enhanced

SUMOylated DELLA abundance (Figure 2E). However GA treatment induced a rapid disappearance of both SUMOylated and non-SUMOylated RGA forms indicating that SUMOylation of DELLAs acts primarily to increase DELLA abundance (Figure S2C, E). This data however does not preclude the possibility that deSUMOylation of RGA must occur prior to its degradation. We next sought to establish the mechanistic role of SUMOylation on DELLA protein accumulation. We previously showed that RGA protein levels are increased in *ots1 ots2* compared to wild type. We further confirmed this was also the case for GFP:RGA fusion proteins by crossing the *pRGA::GFP:RGA* plant lines with *ots1 ots2* mutants. This allowed us to compare GFP:RGA and SUMOylated GFP:RGA protein levels in the presence and absence of OTS1 and OTS2 activities. We observed as expected more SUMOylated GFP:RGA in *ots1 ots2* mutants compared to wild-type and this was associated with higher GFP:RGA levels (Figure 2F and Figure S2D). This effect on SUMOylated and non-SUMOylated GFP:RGA was enhanced when *ots1 ots2* plants were grown in the presence of salt (Figure 2G). Our data indicate that stress-related OTS SUMO proteases are major regulators of DELLA levels *in vivo*.

SUMOylation affects DELLA stability

To elucidate the mechanism for how SUMOylation affects the accumulation of DELLAs in a GA-independent manner, we first produced transgenic plants that over-expressed *OTS1* and *OTS2* in the *gal-5* background (which is partially deficient in bioactive GA and therefore allows accumulation of DELLAs). Over-expression of *OTS1* or *OTS2* SUMO proteases in the *gal-5* genetic background attenuated the growth repression mediated by higher DELLA protein levels in these GA-deficient plants (Figure 3A,

Figure S3A, B and C). Western blot analysis showed a clear decrease in DELLA protein accumulation indicating that continuous deSUMOylation by OTS results in lower DELLA levels (Figure 3B). Conversely *DELLA* transcript levels were up-regulated in *OTS2* overexpressing lines, as a result of an established negative feedback loop initiated by lowering DELLA protein levels (Ariizumi et al., 2008) (Figure 3C). As *gal-5* plants produce very low levels of bioactive GAs it is unlikely that an increase in GA levels can account for this derepression of growth (Figure 3A). Hence, these data provide further evidence for the existence of an alternative mechanism working via SUMOylation that directly modifies DELLA levels.

To test this new DELLA regulatory mechanism further, we produced transgenic plants ectopically expressing either a wild-type copy of RGA fused to GFP (*35S::RGA:GFP*) or mutagenized versions of RGA lacking the relevant SUMO attachment site lysine (*35S::RGA^{K65R}:GFP*) in the *gal-5* genetic background. Surprisingly, unlike *35S::RGA:GFP*, the majority of *35S::RGA^{K65R}:GFP* plants displayed a reduced stature and a slight delay in flowering time (Figure S3D and S3E). Western analysis in T3 lines showed that the K65R form of RGA accumulated at higher levels compared to wild type RGA, despite comparable levels of transgene transcript levels (Figure S3F). These data are indicative of increased DELLA suppressive function conferred by the K65R amino acid substitution in RGA, at least in the *gal-5* background, perhaps owing to reduced *rga^{K65R}* protein turnover. Indeed, the *rga^{K65R}* protein showed increased stability compared to wild-type following cyclohexamide applications (Figure S3F). A reduced turnover of *rga^{K65R}* protein was reflected in the phenotype of heterozygous *GAI/gal-5*

35S::RGA^{K65R}:GFP/- plants, characterised by a decreased GA-dependent growth recovery compared to wild type (Figure S3G).

Intriguingly we notice that among the DELLAs, the SUMO site of RGA is the most divergent in the amino acid immediately N-terminus of the lysine residue (K65) i.e. the first amino acid characterising the SUMOylation motif (which, with the exception of RGA and RGL1, is invariably a glutamine residue in DELLAs, Figure 2D). Because of this, we turned our attention to the GAI protein, more representative of the DELLA SUMOylation motif found in plants. To avoid complex genetic interactions with the *gai* background we analysed transgenic plants expressing high levels of GAI or *gai*^{K49R} fused to the GFP plants in the Columbia wild type background, where GA biosynthesis occurs. The K49R substitution resulted in a dramatically decreased GAI:GFP protein accumulation (Figure 3F) eventhough the transcript levels were comparable to wildtype GAI levels (Figure 3G). This was reflected in reduced DELLA suppressive function, with *35S::GAI^{K49R}:GFP* plants displaying increased root growth compared with *35S::GAI:GFP*, although still significantly reduced compared with wild type (Figure 3D and E). Furthermore, root growth inhibition in *35S::GAI^{K49R}:GFP* plants under salt conditions was significantly ($p < 0.01$, Student *t* Test) less severe than *35S::GAI:GFP* (Figure 3E). Consistent with a reduced suppressive function of the *gai*^{K49R} allele, *35S::GAI^{K49R}:GFP* displayed very similar flowering time compared with wild type (Figure S3H). Our data directly indicates that the SUMOylation of DELLA is crucial for its stability *in planta*.

SUMO interacts with GID1 in a GA independent manner

We next investigated whether the SUMOylated DELLA could interfere with the function of other components of the GA signalling pathway, namely GID1 (Ueguchi-Tanaka et al., 2005) and SLEEPY1 (McGinnis et al., 2003). Closer inspection of the GID1 protein sequence revealed a functional SUMO interaction motif (SIM) at its N-terminus which is widely conserved in plants (Figure 4A, B). In contrast a SIM motif could not be identified in SLEEPY1. We directly demonstrated that recombinant GST-tagged GID1a can bind to SUMO1 in a GA-independent manner in pull down assays (Figure S4A), a result consolidated using surface plasmon resonance (SPR) (Figure 4D). The SIM is identified on the surface of the crystal structure of GID1 where it contributes to the interface which forms the DELLA-binding site (Figure 4C). We then tested whether SUMOylated DELLA had similar GID1a binding properties to uncoupled SUMO1. Recombinant GST-tagged GID1a was incubated with a plant-derived DELLA mixture (consisting of both SUMOylated and non-SUMOylated forms). Using an anti-GST IP, we found that SUMOylated RGA bound to GST:GID1a even in the absence of GA (Figure 4F). Conversely, the binding of non-SUMOylated RGA to GST:GID1a was strictly GA-dependent. The data and the structural model was developed using PyMOL Graphics software based on the previously resolved structures of GID1 and DELLA (Murase et al., 2008) (Figure 4C) suggested that free SUMO and SUMOylated DELLAs compete with DELLAs for GID1 binding. An SPR assay supported this observation (Figure 4E). The results allowed us to postulate that a relatively small pool of SUMOylated DELLA could stabilize the larger pool of unmodified DELLA by titrating out GID1a protein. To test the hypothesis that GID1a protein is rate limiting for DELLA degradation we overexpressed GID1a in *ots1 ots2* double mutant plants where there are higher levels of both

SUMOylated DELLA and non-SUMOylated DELLAs. We anticipated that by overexpressing GID1a we should overcome growth restriction in salt and sensitivity to the GA-biosynthesis inhibitor paclobutrazol (PAC) mediated by increased DELLA levels in the *ots1 ots2* double mutant. The *ots1 ots2* double mutant shows a dramatic delay in germination during PAC treatment (Figure S1A, B and 4G) and is overly sensitive to salt shown by inhibition of primary root growth (Figure S4C; Conti et al., 2008). Both these phenotypes are suppressed when GID1a is overexpressed in this genetic background (Figure 4H, G, S4B and C). Therefore, our data indicates that GID1 is rate limiting in maintaining the steady state levels of DELLA proteins. Furthermore overexpressing a variant GID1a with its SIM site disrupted (GID1a^{V22A}) further enhanced *ots1 ots2* growth under both control and salt conditions compared to the overexpression of wild-type GID1a (Figure 4I and S4D). These data provide crucial genetic evidence that the SIM domain in GID1 is the target for SUMO mediated inhibition of GID1 interaction with DELLAs. Taken together we conclude that SUMO is a novel regulator of DELLA accumulation by altering the availability of GID1 (Figure 4I).

DISCUSSION

Ubiquitination of DELLAs is to date the only peptide modification demonstrated for these proteins, despite the site of ubiquitin attachment being yet unknown. This peptide modification has profound effect on DELLA stability and thus far reaching implications for plant growth regulation. In this study we reveal a new form of peptide modification, SUMOylation. Furthermore we identify the site of SUMO attachment and reveal a novel mechanism of how it stabilises DELLA proteins.

This study highlights the central role of OTS proteases in DELLA SUMOylation control. OTS proteases are rapidly degraded upon salt stress (Conti et al., 2008), thus contributing to hyperSUMOylation/accumulation of DELLAs and consequently causing beneficial growth restraint. SUMOylation may therefore act as a rapid growth retardation mechanism at the onset of stress whilst reduction in GA levels act as a longer-term response, shaping the overall plant growth architecture.

Currently the main strategy used in the transmission of plant hormones signals is to regulate the levels of key repressor or activator proteins using the ubiquitin proteasome system in a hormone concentration dependent manner (Santner et al., 2009). In this context GID1 plays a crucial link between the hormone and ubiquitin-mediated degradation of DELLA repressor proteins. The results reported here support the conclusion that there is an alternative mechanism for DELLA proteins to recognize the GA receptor GID1 via the SIM-SUMO interaction. Our study also establishes that SUMOylation can be recruited to block GID1 receptor access to DELLAs in a novel manner. The GA independent nature of SUMOylated DELLA interaction with GID1 may allow a fast sequestration process, “mopping up” GID1 protein independently of its GA bound state (Figure 4J). We believe that this may represent a failsafe mechanism for DELLA accumulation occurring before a cell activates the relatively slower processes associated with the down regulation of GA during stressed conditions.

The SUMO-SIM interaction is emerging as a key theme in molecular signalling in a wide range of organisms (Geiss-Friedlander and Melchior, 2007). This study describes how the SUMO-SIM ‘molecular glue’ paradigm operates within plants to block ubiquitination of target proteins (i.e. by sequestering the chaperone GID1 needed for ubiquitination of its

target protein DELLA). Interestingly the SIM motif in GID1 that interacts with SUMO1 is located in the N-terminal helical switch region known to bind the VHYNP and LEXLE motifs in DELLA proteins suggesting that SUMO1 may act as a physical barrier for GID1 to bind DELLAs directly (Figure 4C). Furthermore the SIM motif region in GID1 overlaps with the N-terminal ‘lid’ region that covers the GA docking pocket within the receptor. It is therefore tempting to speculate that SUMOylation may also interfere with GA access to GID1 and consequently its binding to the DELLA motif.

DELLAs restrain plant growth, whereas GA promotes growth by targeting the DELLAs for destruction. Different studies have demonstrated that DELLA restraint is a key mechanism for plants to modulate growth according to environmental cues (Achard et al., 2006; 2008a). For example, DELLAs sequester light responsive and phytochrome interacting transcription factors such as PIF3 and PIF4 and inhibit hypocotyl elongation in the light (de Lucas et al., 2008; Feng et al., 2008). Similarly DELLAs also sequester JAZ proteins and prevent their inhibitory effect on the transcription factor MYC2 in root development (Hou et al., 2010). In all these cases the common central thread is the relative abundance of DELLAs, which is modulated by changes in GA levels. We have demonstrated that dwarfism can be reversed independently of GA levels by modifying the SUMOylation status of DELLAs and that this mechanism is particularly important for plant growth under stress. Thus, the discovery of an alternative mechanism regulating DELLA abundance reported in this study provides an important new insight into the integrative role of DELLAs in controlling plant growth.

EXPERIMENTAL PROCEDURE

Plant material and growth conditions

Unless specifically stated, plants used in this study were in the Col-0 background with the exception for *pRGA::GFP:RGA* which is in the Landsberg *erecta*. Multiple mutants were generated by crossing. Transgenic plants were obtained by transformation of the relevant genetic background by floral dipping (Clough and Bent, 1998). *35S::RGA:GFP gal-5* and *35S::RGA^{K65R}:GFP gal-5* plants were compared with a vector only control (*gal-5*) by selecting of 15 to 25 independent T1 Basta resistant plants. Further analysis was done on homozygous T3 and T4 lines showing stable levels of expression. Several (12 each) *35S::GAI:GFP* and *35S::GAI^{K49R}:GFP* lines were isolated in the Col-0 background. Homozygous T3 and T4 lines with high levels of expression were selected for molecular and phenotypic analysis. For the OTS1/2 overexpression in the *gal-5* background, a total of 21 T1 lines (14 *OTS2* and 7 for *OTS1*) were isolated and T2 seeds lines analyzed for phenotype and expression levels. 12 GID1:TAPtag lines were isolated (both in the WT Col-0 or *ots1 ots2*). 5 T3 and T4 were analyzed further for expression as detailed by immunoblot in Fig. S4B. T-DNA lines seeds were obtained from the Nottingham Arabidopsis stock centre. The *ots1-1 ots2-1* double mutants plants were previously described (Conti et al., 2008). The *ots2-2* mutant is a novel T-DNA insertion allele (SALK_067439) resulting in no detectable full length *OTS2* transcript. The *ots2-2* allele was detected by PCR on genomic DNA using primers LC15 and LC18, flanking the T-DNA insertion region and LBa1 (SALK T-DNA primer) in combination with LC15, which were insertion-specific. The null *rga* mutant allele used in this study (dubbed *rga-100*) derives from a T-DNA insertion (SALK_089146C). Homozygous plants were genotyped with primers LC69 and LC70, flanking the T-DNA insertion region and LBa1

(SALK T-DNA primer) and LC70, which were insertion allele specific. The null *gai* mutant allele used in this study (dubbed *gai-100*) derived from a T-DNA insertion (SAIL_587_C02). Homozygous plants were resistant to the herbicide Basta and confirmed by PCR using with primers LC80 and LC81, flanking the T-DNA insertion region and LB1 (SAIL T-DNA primer) and LC81, which were insertion allele specific. The *gai-5* mutants were obtained from NASC and the *pRGA::GFP:RGA* line (Silverstone et al., 2001), *35S::NPR1:GFP npr1* (Kinkema et al., 2000) plants were previously described. The *pRGA::GFP:RGA ots1 ots2* line derives from a cross between *ots1 ots2* (Col-0) and the *pRGA:GFP-RGA* (*Ler*). OTS1 OTS2 and *ots1 ots2* F2 plants (Col-0/*Ler*) carrying the *pRGA::GFP:RGA* transgene were isolated. These were next made homozygous for the *pRGA::GFP:RGA* transgene.

The procedures for Arabidopsis plant growth were previously described (Conti et al., 2008). GA quantification was conducted from tissue deriving from young seedlings (10 days) grown in plant growth medium plate. GA measurements were done as previously illustrated (Griffiths et al., 2006). For the germination assay, GA₃ and PAC were supplemented to the plant growth medium (half strength Murashige and Skoog – Sigma-, 0.5% Sucrose, 1% Agar). Seeds were stratified on plates for three days before exposure to light and scored after 3 to 5 days. For proteins and transcripts analysis, surface sterilised seeds were stratified and germinated on filter papers laid on plant agar growth medium and pooled seedlings (20-40) were harvested after 8 to 10 days.

Plasmid construction

All constructs were made by recombining entry clones to GATEWAY destination vectors via LR Recombinase II (Invitrogen). The *35S::3XHA:OTS1* and *35S::4Xmyc:OTS2* constructs were generated by recombining the plasmids pLCG1 and pLCG14 (Conti et al., 2008) (harbouring the *OTS1* and *OTS2* cDNAs, respectively) with the binary vectors pGWB15 and pGWB18 (respectively) (Nakagawa et al., 2007). The *RGA* ORF (and part of the 5' UTR region) was amplified by PCR from whole cDNAs from seedlings with oligos LC75 and LC76 and cloned into pENTR/D-TOPO (Invitrogen) to yield pLCG67. The *GAI* ORF was amplified by PCR from a plasmid template, with oligos LC80 and LC81 and cloned into pENTR/D-TOPO (Invitrogen) to yield pLCG69. The *rga*^{K65R} and *gai*^{K49R} alleles were generated by amplifying pLCG67 and pLCG69 with mutagenic oligos LC77/LC78 and LC71/LC72, respectively (which carried a single base pair change) according to the QuikChange Site-Directed Mutagenesis Kit Directions (Stratagene) and the resulting plasmid (pLCG68, *rga*^{K65R} and pLCG78, *gai*^{K49R}) were confirmed by sequenced. Overexpression constructs were generated by recombining the plasmids pLCG67, pLCG68, pLCG69 and pLCG78 with destination vector pGBPGWG (Zhong et al., 2008).

The *GID1a* ORF was amplified by PCR from whole cDNAs from seedlings with oligos LC73 and LC74 and cloned into pENTR/D-TOPO (Invitrogen) to yield pLCG66. The *35S::GID1a:TAP* construct were generated by recombining the plasmids pLCG66 with the binary vector pEarleyGate 205 (Earley et al., 2006). For SPR-based and GST binding assays, the fusion *GST:GID1a* construct was generated by recombining the plasmids pLCG66 with the destination vector pDEST15. *RGA* (pLCG67) was cloned into pET 55

DEST (Millipore) to introduce a C-terminal His tag. GAI (pLCG68) was recombined with pDEST15 to yield a GST:GAI fusion.

Full details of the primers used in this study are listed in Supplementary Table 1.

Protein extraction, immunoprecipitation and antibodies

Total proteins were extracted by homogenizing fresh *Arabidopsis* seedlings in the presence of ice cold extraction buffer as previously described (Conti et al., 2008). The homogenates were clarified by spinning 10 min at 4°C at $16000 \times g$ and the supernatant quantified with the Bradford assay. Approximately 2-3 mg were subjected to immunoprecipitation using the GFP Isolation Kit (Chromotek) according to the manufacturers' instructions. GFP beads were washed four times with extraction buffer and once with 20 mM tris HCl, pH 7.5 before elution with hot SDS-PAGE buffer (50 mM tris HCl, pH 6.8, 50 mM DTT, 1% SDS, 1 mM EDTA, 0.005% bromphenol blue, 10% glycerol). For combined RNA and protein analysis, the protein fraction was obtained by following the TRIzol (life technologies) reagent protocol. The isopropanol precipitated protein pellet was washed three times in 0.3 M guanidine hydrochloride, 95% ethanol before solubilisation in 6 M urea, 0.1% SDS. Total proteins were quantified with the Bradford reagent and an equal amount of proteins was precipitated with five volumes of cold acetone. The pellet was then resuspended in SDS-PAGE loading buffer (containing urea 4 M) before loading. To reveal the SUMOylation pattern at high resolution, the immunoprecipitates were resolved on precast 4-8% Tris-Acetate NuPAGE gels (Invitrogen) otherwise proteins (50-100 µg) were resolved on standard 8% SDS-PAGE gels. Proteins were blotted and probed with *At*SUMO1 and TAPtag antibodies as

previously described (Conti et al., 2008). The RGA and GAI antibodies were made in sheep and used at a 1:2000 dilution. The rabbit GFP and GST antibodies were bought from abcam and used at a 1:4000 dilution.

Recombinant proteins and GST pull down assay

Recombinant OTS1 protein expression and production in *E. coli* were previously described (Conti et al., 2008). RGA (RGA:His) and GID1a (GST:GID1a) were expressed in *E. coli* CodonPlus RIL (DE3) cells (Agilent), while GST and His:*AtSUMO1* (Okada et al., 2009) were expressed in BL21 (DE3) cells. Cells were grown in LB cultures at 37°C to an $OD_{600} = 1.0$ and protein expression induced by adding isopropyl- β -D-thiogalactopyranoside (IPTG, 0.1 mM) for 4 hours at 30°C. The pellets containing RGA:His and His:*AtSUMO1* were resuspended in His lysis buffer (20 mM sodium phosphate pH 7.4, 0.5 M NaCl, 20 mM imidazole, 100 μ g/ml lysozyme, 250 U/ml Benzonase, Novagen, 1X Complete EDTA-free Protease Inhibitor cocktail, Roche). The GST:GID1a and GST pellets were resuspended in GST lysis buffer (12 mM sodium phosphate pH 7.4, 140 mM NaCl, 2.7 mM KCl, 100 μ g/ml lysozyme, 250 U/ml Benzonase, 1x Complete EDTA-free Protease Inhibitor cocktail). Cells were lysed by sonication on ice and the lysate was agitated at 25°C for 10 minutes. After centrifugation (27000 \times g, 15 minutes, 0°C), the supernatants were passed through a 0.2 μ m filter. Tagged proteins were purified using HisTrap HP or GSTrap HP columns (GE Healthcare) on an ÄKTA purifier system (GE Healthcare) as per column instructions. Eluted proteins were dialysed against 10 mM HEPES pH 8.0, 150 mM NaCl, 1 mM EDTA and their concentration adjusted to 1 mg/ml.

The GST pull down assay was done by mixing affinity purified GST:GID1a (0.1 μg) or GST with His:*At*SUMO1 (0.1 μg) and incubation in 1X reaction buffer (Gamborg's B5 – minimal organics, 50 mM NaCl, 0.05% Igepal CA-630, 1 mM DTT, 50 mM tris HCl, pH 7.5). GA₃ was added at a final concentration of 10 μM . Proteins were pulled-down using the GST Isolation Kit, according to the manufacturer's instruction (Millipore). Plant GFP:RGA proteins were affinity captured as previously described and eluted from anti-GFP beads with 0.1 % triethanolamine, 0.1% Triton X100 and neutralised with 100 mM MES (pH 2.5). The eluate was dialyzed against 50 mM tris HCl, pH 7.5, 50 mM NaCl, 1mM DTT. Plant purified GFP:RGA proteins were split into different tubes and incubated with recombinant GST:GID1a (0.1 μg) or GST proteins in 1X reaction buffer (with freshly added protease inhibitor cocktail) in the presence or absence of 10 μM GA₃. GST-bound proteins were pulled-down using the GST Isolation Kit, washed four times with 1X reaction buffer and eluted according to the manufacturers' instruction.

Surface Plasmon Resonance

SPR was carried out on a Biacore 2000 instrument at 25°C. Purified GID1a was amine-coupled to a CM5 sensor chip (GE Healthcare). Flow cell 1 was blocked using ethanolamine and used as reference. Approx 500 RU of GID1a was bound to flow cells 2 and 3. All binding assays were carried out in HBS-EP buffer (10 mM HEPES pH 7.5, 150 mM NaCl, 1mM EDTA, 1mM DTT, 0.005% P20) at a flow rate of 20 $\mu\text{l}/\text{min}$ using 180 second injections followed by 180s of dissociation in HBS-EP. Each condition was run in duplicate using proteins at 100 $\mu\text{g}/\text{ml}$ in HBS-EP (containing 100 μM GA₃ as appropriate). Regeneration used 10 mM glycine pH 1.5 at 30 $\mu\text{l}/\text{min}$ for 30 s.

Far-western assay

Peptides corresponding to the putative SIMs in GID1 were purchased from Cambridge Research Biochemicals. 1 µg of each peptide was spotted on a nitrocellulose membrane and allowed to dry. Membranes were equilibrated in TBST (25 mM tris HCl, pH . 7.4, 150 mM NaCl, 0.1% Tween 20). Peptides were probed for 1 hour with recombinant His:AtSUMO1 (10 µg/ml) in TBST-milk 5%, washed and subsequently probed with SUMO1 antibodies for standard chemilluminescence based detection.

On-column deSUMOylation assay

GFP:RGA proteins were affinity captured from total proteins extracts of *pRGA::GFP:RGA* transgenic plants with the µMACS GFP Isolation Kit. Magnetic beads were eluted from the columns with 50 µl of 20 mM tris HCl, pH 7.5 and split into different tubes. Purified GFP:RGA proteins were incubated with 5-10 µg of recombinant OTS1 or OTS1^{C526S}, or 300 ng of GST tagged human SENP1 or SENP2 (catalytic domain) (Bailey and O'Hare, 2004) (Enzo life sciences). After incubation (typically 1-2 hours at room temperature), the beads were applied to the column, washed and bound proteins eluted with SDS-PAGE loading buffer.

Transcript analysis

Plant material (young seedlings) was pulverized with a pestle in the presence of liquid nitrogen and total RNA was extracted with the TRIzol reagent (life technologies). First strand cDNA synthesis was carried out from 500 ng of total RNA using the VILO reverse

transcriptase kit (Invitrogen). cDNA was diluted 5 times, mixed with the FAST Sybr Green master mix (Applied Biosystem) and used for qPCR with a 7900HT Fast Real-time PCR (Applied Biosystem). To detect *RGA* transcript levels, oligonucleotides lcm26 and lcm27 were used; for *GAI*, oligonucleotides lcm28 and lcm29. *OTS2* transcript levels were analysed using oligonucleotides LC85 and LC86. The primers for detecting *GA3ox1* (Zentella et al., 2007), *GA20ox2* (Achard et al., 2008a), *GA2ox6* (Griffiths et al., 2006) and *GA2ox2* (Rieu et al., 2008) were previously described. Oligonucleotides mr37 and mr38 amplifying *ACT2* (At3g18780) were used for normalization. Changes in gene expression were calculated relative to *ACT2* using the $\Delta\Delta\text{Ct}$ method (Livak and Schmittgen, 2001).

REFERENCES

- Achard, P., Cheng, H., De Grauwe, L., Decat, J., Schoutteten, H., Moritz, T., Van Der Straeten, D., Peng, J., and Harberd, N.P. (2006). Integration of plant responses to environmentally activated phytohormonal signals. *Science* *311*, 91–94.
- Achard, P., Gong, F., Cheminant, S., Alioua, M., Hedden, P., and Genschik, P. (2008a). The cold-inducible CBF1 factor-dependent signaling pathway modulates the accumulation of the growth-repressing DELLA proteins via its effect on gibberellin metabolism. *Plant Cell* *20*, 2117–2129.
- Achard, P., Renou, J.-P., Berthomé, R., Harberd, N.P., and Genschik, P. (2008b). Plant DELLAs restrain growth and promote survival of adversity by reducing the levels of reactive oxygen species. *Curr. Biol.* *18*, 656–660.
- Ariizumi, T., Murase, K., Sun, T.-P., and Steber, C.M. (2008). Proteolysis-independent downregulation of DELLA repression in Arabidopsis by the gibberellin receptor GIBBERELLIN INSENSITIVE DWARF1. *Plant Cell* *20*, 2447–2459.
- Asako Shimada, Ueguchi-Tanaka, M., Toru Nakatsu, Nakajima, M., Youichi Naoe, Hiroko Ohmiya, Hiroaki Kato, and Matsuoka, M. (2008). Structural basis for gibberellin recognition by its receptor GID1. *Nature* *456*, 520–523.
- Bailey, D., and O'Hare, P. (2004). Characterization of the localization and proteolytic activity of the SUMO-specific protease, SENP1. *J. Biol. Chem.* *279*, 692–703.

Clough, S.J., and Bent, A.F. (1998). Floral dip: a simplified method for *Agrobacterium*-mediated transformation of *Arabidopsis thaliana*. *Plant J* *16*, 735–743.

Conti, L., Price, G., O'Donnell, E., Schwessinger, B., Dominy, P., and Sadanandom, A. (2008). Small ubiquitin-like modifier proteases OVERLY TOLERANT TO SALT1 and -2 regulate salt stress responses in *Arabidopsis*. *Plant Cell* *20*, 2894–2908.

de Lucas, M., Davière, J.-M., Rodríguez-Falcón, M., Pontin, M., Iglesias-Pedraz, J.M., Lorrain, S., Fankhauser, C., Blázquez, M.A., Titarenko, E., and Prat, S. (2008). A molecular framework for light and gibberellin control of cell elongation. *Nature* *451*, 480–484.

Dill, A., and T Sun (2001). Synergistic derepression of gibberellin signaling by removing RGA and GAI function in *Arabidopsis thaliana*. *Genetics* *159*, 777–785.

Earley, K.W., Haag, J.R., Pontes, O., Opper, K., Juehne, T., Song, K., and Pikaard, C.S. (2006). Gateway-compatible vectors for plant functional genomics and proteomics. *Plant J* *45*, 616–629.

Feng, S., Martínez, C., Gusmaroli, G., Wang, Y., Zhou, J., Wang, F., Chen, L., Yu, L., Iglesias-Pedraz, J.M., Kircher, S., et al. (2008). Coordinated regulation of *Arabidopsis thaliana* development by light and gibberellins. *Nature* *451*, 475–479.

Fu, X., Donald E Richards, Ait-Ali, T., Hynes, L.W., Ougham, H., Peng, J., and Harberd, N.P. (2002). Gibberellin-mediated proteasome-dependent degradation of the barley DELLA protein SLN1 repressor. *Plant Cell* *14*, 3191–3200.

Fu, X., Donald E Richards, Fleck, B., Xie, D., Burton, N., and Harberd, N.P. (2004). The *Arabidopsis* mutant *sleepy1gar2-1* protein promotes plant growth by increasing the affinity of the SCFSLY1 E3 ubiquitin ligase for DELLA protein substrates. *Plant Cell* *16*, 1406–1418.

Geiss-Friedlander, R., and Melchior, F. (2007). Concepts in sumoylation: a decade on. *Nat Rev Mol Cell Biol* *8*, 947–956.

Griffiths, J., Murase, K., Rieu, I., Zentella, R., Zhang, Z.-L., Powers, S.J., Gong, F., Phillips, A.L., Hedden, P., Sun, T.-P., et al. (2006). Genetic characterization and functional analysis of the GID1 gibberellin receptors in *Arabidopsis*. *Plant Cell* *18*, 3399–3414.

Hou, X., Lee, L.Y.C., Xia, K., Yan, Y., and Yu, H. (2010). DELLAs modulate jasmonate signaling via competitive binding to JAZs. *Dev Cell* *19*, 884–894.

Ikeda, A., Ueguchi-Tanaka, M., Sonoda, Y., Kitano, H., Koshioka, M., Futsuhara, Y., Matsuoka, M., and Yamaguchi, J. (2001). *slender rice*, a constitutive gibberellin response mutant, is caused by a null mutation of the SLR1 gene, an ortholog of the height-regulating gene GAI/RGA/RHT/D8. *Plant Cell* *13*, 999–1010.

Itoh, H., Ueguchi-Tanaka, M., Sato, Y., Ashikari, M., and Matsuoka, M. (2002). The Gibberellin Signaling Pathway Is Regulated by the Appearance and Disappearance of SLENDER RICE1 in Nuclei. *Plant Cell* 14, 57.

Kinkema, M., Fan, W., and Dong, X. (2000). Nuclear localization of NPR1 is required for activation of PR gene expression. *Plant Cell* 12, 2339–2350.

Lee, M.H., Lee, S.W., Lee, E.J., Choi, S.J., Chung, S.S., Lee, J.I., Cho, J.M., Seol, J.H., Baek, S.H., Kim, K.I., et al. (2006). SUMO-specific protease SUSP4 positively regulates p53 by promoting Mdm2 self-ubiquitination. *Nat. Cell Biol.* 8, 1424–1431.

Lee, S., Cheng, H., King, K.E., Wang, W., He, Y., Hussain, A., Lo, J., Harberd, N.P., and Peng, J. (2002). Gibberellin regulates Arabidopsis seed germination via RGL2, a GAI/RGA-like gene whose expression is up-regulated following imbibition. *Genes Dev.* 16, 646–658.

Livak, K.J., and Schmittgen, T.D. (2001). Analysis of relative gene expression data using real-time quantitative PCR and the 2(-Delta Delta C(T)) Method. *Methods* 25, 402–408.

McGinnis, K.M., Thomas, S.G., Soule, J.D., Strader, L.C., Zale, J.M., Sun, T.-P., and Steber, C.M. (2003). The Arabidopsis SLEEPY1 gene encodes a putative F-box subunit of an SCF E3 ubiquitin ligase. *Plant Cell* 15, 1120–1130.

Miura, K., Lee, J., Jin, J.B., Yoo, C.Y., Miura, T., and Hasegawa, P.M. (2009). Sumoylation of ABI5 by the Arabidopsis SUMO E3 ligase SIZ1 negatively regulates abscisic acid signaling. *Proc Natl Acad Sci USA* 106, 5418–5423.

Murase, K., Yoshinori Hirano, Sun, T.-P., and Toshio Hakoshima (2008). Gibberellin-induced DELLA recognition by the gibberellin receptor GID1. *Nature* 456, 459–463.

Nakagawa, T., Kurose, T., Hino, T., Tanaka, K., Kawamukai, M., Niwa, Y., Toyooka, K., Matsuoka, K., Jinbo, T., and Kimura, T. (2007). Development of series of gateway binary vectors, pGWBs, for realizing efficient construction of fusion genes for plant transformation. *J. Biosci. Bioeng.* 104, 34–41.

Navarro, L., Bari, R., Achard, P., Lisón, P., Nemri, A., Harberd, N.P., and Jones, J.D.G. (2008). DELLAs control plant immune responses by modulating the balance of jasmonic acid and salicylic acid signaling. *Curr. Biol.* 18, 650–655.

Okada, S., Nagabuchi, M., Takamura, Y., Nakagawa, T., Shinmyozu, K., Nakayama, J.-I., and Tanaka, K. (2009). Reconstitution of Arabidopsis thaliana SUMO pathways in E. coli: functional evaluation of SUMO machinery proteins and mapping of SUMOylation sites by mass spectrometry. *Plant Cell Physiol* 50, 1049–1061.

Peng, J., Carol, P., Richards, D.E., King, K.E., Cowling, R.J., Murphy, G.P., and Harberd, N.P. (1997). The Arabidopsis GAI gene defines a signaling pathway that negatively regulates gibberellin responses. *Genes Dev.* 11, 3194–3205.

Peng, J., Donald E Richards, Nigel M Hartley, George P Murphy, Katrien M Devos, John E Flintham, James Beales, Leslie J Fish, Anthony J Worland, Fatima Pelica, et al. (1999). Green revolution genes encode mutant gibberellin response modulators. *Nature* 400, 256.

Reeves, P.H., Murtas, G., Dash, S., and Coupland, G. (2002). early in short days 4, a mutation in *Arabidopsis* that causes early flowering and reduces the mRNA abundance of the floral repressor FLC. *Development* 129, 5349–5361.

Rieu, I., Eriksson, S., Powers, S., Gong, F., Griffiths, J., Woolley, L., Benlloch, R., Nilsson, O., Thomas, S., Hedden, P., et al. (2008). Genetic Analysis Reveals That C19-GA 2-Oxidation Is a Major Gibberellin Inactivation Pathway in *Arabidopsis*. *Plant Cell* 20, 2420–2436.

Santner, A., Santner, A., Estelle, M., and Estelle, M. (2009). Recent advances and emerging trends in plant hormone signalling. *Nature* 459, 1071.

Silverstone, A.L., Jung, H.S., Dill, A., Kawaide, H., Kamiya, Y., and Sun, T.P. (2001). Repressing a repressor: gibberellin-induced rapid reduction of the RGA protein in *Arabidopsis*. *Plant Cell* 13, 1555–1566.

Silverstone, A.L., Mak, P.Y., Martínez, E.C., and Sun, T.P. (1997). The new RGA locus encodes a negative regulator of gibberellin response in *Arabidopsis thaliana*. *Genetics* 146, 1087–1099.

Tyler, L., Thomas, S.G., Hu, J., Dill, A., Alonso, J.M., Ecker, J.R., and Sun, T.-P. (2004). DELLA proteins and gibberellin-regulated seed germination and floral development in *Arabidopsis*. *Plant Physiol.* 135, 1008–1019.

Ueguchi-Tanaka, M., Ashikari, M., Nakajima, M., Itoh, H., Katoh, E., Kobayashi, M., Chow, T.-Y., Hsing, Y.-I.C., Kitano, H., Yamaguchi, I., et al. (2005). GIBBERELLIN INSENSITIVE DWARF1 encodes a soluble receptor for gibberellin. *Nature* 437, 693–698.

Ueguchi-Tanaka, M., Nakajima, M., Katoh, E., Hiroko Ohmiya, Asano, K., Saji, S., Hongyu, X., Ashikari, M., Kitano, H., Yamaguchi, I., et al. (2007). Molecular interactions of a soluble gibberellin receptor, GID1, with a rice DELLA protein, SLR1, and gibberellin. *Plant Cell* 19, 2140–2155.

Wang, F., Zhu, D., Huang, X., Li, S., Gong, Y., Yao, Q., Fu, X., Fan, L.-M., and Deng, X.-W. (2009). Biochemical insights on degradation of *Arabidopsis* DELLA proteins gained from a cell-free assay system. *Plant Cell* 21, 2378–2390.

Willige, B.C., Ghosh, S., Nill, C., Zourelidou, M., Dohmann, E.M.N., Maier, A., and Schwechheimer, C. (2007). The DELLA domain of GA INSENSITIVE mediates the interaction with the GA INSENSITIVE DWARF1A gibberellin receptor of *Arabidopsis*. *Plant Cell* 19, 1209–1220.

Zentella, R., Zhang, Z.-L., Park, M., Thomas, S.G., Endo, A., Murase, K., Fleet, C.M.,

Jikumaru, Y., Nambara, E., Kamiya, Y., et al. (2007). Global analysis of della direct targets in early gibberellin signaling in Arabidopsis. *Plant Cell* *19*, 3037–3057.

Zhong, S., Zhong, S., Lin, Z., Lin, Z., Fray, R.G., Fray, R.G., Grierson, D., and Grierson, D. (2008). Improved plant transformation vectors for fluorescent protein tagging. *Transgenic Research* *17*, 985–989.

AKNOLWDGEMENTS

L.C. was supported by a research fellowship from the Biological and Biotechnological Research Council (BBSRC), the University of Milan and the Leverhulme Trust. S.N. was supported by a studentship from the BBSRC, which also provided grant-aided support to Rothamsted Research. This work was also supported by the Fondazione Umberto Veronesi, Milan (project AGRISOST) and by a MIUR PRIN project (2010-2011 prot. 2010HEBBB8_006) to MB and CT.

We would like to acknowledge Professor Nicholas Harberd for providing the GAI clone and *pRGA::GFP:RGA* transgenic lines and Dr Fan Gong (Rothamsted Research) for the GA analysis.

FIGURE LEGENDS

Figure 1. OTS1 and OTS2 modulate growth on salt through a DELLA-dependent mechanism.

(A) Image of representative 10 days old seedlings grown in petri dishes in the presence of salt (NaCl). Bar = 5 mm.

(B) Mean root growth of 10 days old seedlings in the presence of 100 mM NaCl expressed as growth (%) relatively to the untreated controls. Error bar = SEM. n = 20-24.

(C) Accumulation of endogenous RGA (top) and GAI (bottom) proteins in 10 days old seedlings grown in petri dishes in the absence (-) or presence (+) of 100 mM NaCl. Number indicates molecular mass (kDa). Coomassie Blue filter staining (C. Blue) serves as a loading control.

(D) Mean levels of Gibberellic Acid (GA) isoforms in *ots1 ots2* double mutants compared with wild type (Col-0). Error bars = SD of 3 biological replicates.

Figure 2. SUMOylation is a novel DELLA peptide modification affecting DELLA accumulation.

(A) Immunoprecipitations (IP aGFP) of total proteins (input) derived from *pRGA::GFP:RGA* or wild-type (*Ler* WT) seedlings. Proteins were probed with GFP (WB aGFP) or *AtSUMO1* (WB a*AtSUMO1/2*) antibodies. Numbers indicate molecular mass (kDa), arrow, the GFP:RGA protein, vertical bars, the SUMOylated forms (S1-GFP:RGA) of GFP:RGA protein.

(B) *in vitro* deSUMOylation of plant-derived SUMOylated GFP:RGA proteins after incubation with OTS1 (His:OTS1) or catalytically-inactive OTS1 (His:OTS1^{C526S}) recombinant proteins.

(C) His:RGA SUMOylation in *E.coli* by activating (E1), conjugating (E2) enzymes and active (His:*AtS1*^{GG}) but not inactive (His:*AtS1*^{AA}) *AtSUMO1*. His:RGA^{K65R} is not SUMOylated. Numbers indicate molecular mass (kDa), arrows, the SUMOylated forms of His:RGA protein. Western Blot is conducted with RGA antibodies (WB aRGA).

(D) Cross-species alignment of the DELLA domain. In bold characters are the conserved lysine residues. The shaded area represents a non-canonical SUMOylation motif.

(E) Pattern of SUMOylated GFP:RGA (left) or GAI:GFP (right) accumulation in *pRGA::GFP:RGA* or *35S::GAI:GFP* seedlings, respectively, grown for 10 days in the absence (-) or presence (+) of NaCl (100 mM). Total proteins (input) were immunoprecipitated with GFP antibodies (IP aGFP) and probed with GFP (WB aGFP) or *AtSUMO1* (WB a*AtS1*) antibodies. Numbers indicate molecular mass (kDa), Coomassie Blue filter staining (C. Blue) serves as a loading control.

(F) Immunoprecipitation (IP aGFP) from total proteins (input) derived from *pRGA::GFP:RGA* seedlings in the wild-type (*OTS1 OTS2*) or mutants (*ots1 ots2*) backgrounds.

(G) Accumulation of GFP:RGA proteins in 10 days old *pRGA::GFP:RGA* seedlings in the wild-type (*OTS1 OTS2*) or mutants (*ots1 ots2*) backgrounds grown in petri dishes in the presence of different concentrations of NaCl. Non-transgenic, wild-type extracts (Col-0) serve as a negative control. Coomassie Blue filter staining (C. Blue) serves as a loading control.

Figure 3. DELLA deSUMOylation impairs DELLA accumulation.

(A) Image of 20 days-old seedlings grown in petri dishes.

(B) Accumulation of endogenous RGA or GAI proteins in 9 days old wild-type (*Ler*), *gal-5* or three independent transgenic (T2) *35S::4Xmyc:OTS2 gal-5* lines seedlings. Western Blot is conducted with RGA or GAI antibodies (WB aRGA, aGAI). RGA* indicates a cross reaction of the GAI antibody with RGA protein. Coomassie Blue filter staining (C. Blue) serves as a loading control.

(C) Real-time PCR analysis of *RGA*, *GAI* and *OTS2* transcripts levels. Total RNA derived from the same material as in (B). Bars indicate the expression levels as fold change variations relatively to *gal-5* (which was arbitrarily set as 1). *ACTIN* was used for normalisation, error bars = SD of two technical replicates.

(D) Image of representative 16 days old transgenic (T4) seedlings of the indicated genotypes (*Col-0* background) grown in control or 100 mM NaCl – containing medium for 8 days.

(E) Mean root growth of 16 days old seedlings of the indicated genotypes expressed as absolute values \pm SD (left) or as growth (%) relatively to the untreated controls \pm SE. Seedlings were transferred to 100 mM NaCl or control plates 8 days after germination. Root length was measured 8 days after transfer. Shown is the mean value for three biological replicates, n = 3-4 plants per replicate.

(F) Accumulation of GAI:GFP or *gai*^{K49R}:GFP proteins in 16 days old transgenic seedlings grown in petri dishes. Non-transgenic, wild-type extracts (*Col-0*) serve as a negative control. Coomassie Blue filter staining (C. Blue) serves as a loading control. Western Blot is conducted with GFP antibodies (WB aGFP). Non-transgenic, wild-type extracts (*Col-0*) serve as a negative control. Asterisk indicates a cross-reacting band detected by the GFP antibody.

(G) Reverse Transcriptase (RT) – PCR analysis of *GFP* transcript levels in transgenic plants shown in (F). *ACTIN* was used for normalization. PCR fragments were resolved on an agarose gel and visualized with ethidium bromide staining under UV light.

Figure 4. SUMOylated DELLA binds GID1 through a SIM and independently from GA.

(A) Cross-species alignment of SIM B (shaded amino acids) in the GID1 protein amino terminal extension (grey).

(B) Far western assay with peptides corresponding to SIM A and SIM B located in the GID1a N-terminal extension. SIMs contain a central hydrophobic core (bold character). The amino acid substitution peptide SIM B^{V22A} results in a strongly reduced SIM-SUMO1 interaction.

(C) Top view of the GID1a N terminal extension (Purple). The SIM B motif (yellow) resides at the interface between GID1a (lavender) and the GAI DELLA domain (green). The position of the GAI SUMOylation site (K49) is shown with a red dot.

(D) Sensorgram of interaction between SUMO1 (*AtS1*) with GID1a. Figure shows binding and saturation of *AtS1* to GID1a followed by disassociation when *AtS1* is removed from buffer flow over GID1a. Shaded area shows SE (standard error of the mean).

(E) Interaction between RGA alone with GID1a (red) and, RGA and SUMO1 (*AtS1*, blue) with GID1a both in the presence of GA₃. The combined response (blue) is reduced in the presence of *AtS1* indicating that less of the higher molecular weight RGA is bound, being displaced by the lower molecular weight *AtS1*. Shaded area shows SE (standard error of the mean).

(F) GST pull down assay between plant-derived GFP:RGA proteins with recombinant GST:GID1a or GST in the presence (+) or absence (-) of GA₃ (10 μM). Pulled-down proteins were probed with *AtSUMO1* (WB a*AtS1*), upper panel, GFP (WB aGFP) middle panel, or GST (WB aGST), lower panel antibodies, respectively.

(G) Mean germination rates (percentage of visible green cotyledons relatively to total number of seeds) under different PAC concentrations of wild type (wt, Col-0), *ots1 ots2* double mutants and six independent transgenic lines (T4) ectopically expressing *GID1a* (*35S::GID1a:TAP*) in the wild-type or *ots1 ots2* backgrounds. Seeds (n= 40-80 for each treatment / genotype combination) were scored 3 days after sowing. Error bars = SD of three biological replicates.

(H) Images of representative 10 days old seedlings grown in petri dishes in the presence or absence of 100 mM salt (NaCl).

(I) Images of representative 8 days old seedlings grown in petri dishes in the presence or absence of 100 mM salt (NaCl).

(J) Model for the SUMOylation-dependent DELLA accumulation in Arabidopsis. In the absence of GA, the SUMOylated (S1, red) pool of DELLA (green), sequester the GA receptor GID1 (purple) through interaction with the SIM motif (yellow) located in the lid region of GID1 (lavender). This allows accumulation of DELLA proteins. In the presence of GA, the GID1-GA complex binds DELLA and in the presence of SLEEPY1 (SLY), targets it for Ubiquitin (Ub)-mediated proteosomal degradation.

SUPPLEMENTARY INFORMATION

Supplementary Figure 1. OTS1 and OTS2 mediate GA signalling through DELLA without changes in *DELLA* transcripts levels.

(A) *ots1 ots2* double mutants are more sensitive to paclobutrazol (PAC) compared with wild type (Col-0). Seeds were photographed 5 days after sowing.

(B) and **(C)** Mean germination rates (percentage of visible green cotyledons relatively to total number of seeds) under different PAC or PAC and/or gibberellic acid (GA₃) concentrations. Seeds (n= 40-80 for each treatment / genotype combination) were scored 3 days after sowing. Error bar = SD of three biological replicates.

(D) Real-time PCR analysis of *RGA* and *GAI* transcripts levels in the indicated genotypes. Total RNA derived from 9 days old seedlings grown in petri dishes in the presence or absence of 100 mM NaCl. Bars indicate the expression levels as fold change variations relatively to wild-type control samples (which was arbitrarily set as 1). *ACTIN* was used for normalisation, error bars = SD of two biological replicate, each one performed in two technical replicates. ND = not detected.

(E) Real-time PCR analysis of GA biosynthetic enzymes transcripts levels from total RNA as in **(D)**. Bars indicate the expression levels as fold change variations relatively to wild-type control samples (which was arbitrarily set as 1). *ACTIN* was used for normalisation, error bars = SD of two to three biological replicates, each one performed in two technical replicates.

(F) Image of four-week-old plants grown under a long day (LD) photoperiod. Arrowhead indicates the presence of an inflorescence. Lower panel, mean number of vegetative

leaves (VL) and cauline leaves (CL) in LD-grown plants scored after bolting. Error bars = SEM, n = 12-15 for each genotype.

Supplementary Figure 2. RGA and GAI are SUMOylated *in vivo*.

(A) Immunoprecipitation (IP aGFP) of total proteins (input) derived from *35S::GFP* or *35S::GFP:NPR1* (*NON EXPRESSER OF PR GENES*) young seedlings sprayed with 1 mM Salicylic acid (+ SA) or control (-SA). Proteins were probed with GFP (WB aGFP) or *AtSUMO1* (WB a*AtS1*) antibodies. Numbers indicate molecular mass (kDa), arrowhead, the GFP:NPR1 or GFP proteins. Ponceau staining of the Rubisco large subunit afforded a loading control.

(B) *in vitro* deSUMOylation of plant-derived SUMOylated GFP:RGA proteins after incubation with recombinant SUMO protease subunits of SENP1 (GST:SENP1) and SENP2 (GST:SENP2) compared with buffer control.

(C) Immunoprecipitation (IP aGFP) of total proteins (input) derived from *pRGA::GFP:RGA* seedlings, harvested at different time point (hours) after being sprayed with GA₃ (100 μM) and compared to untreated control (ctrl). Proteins were probed with GFP (WB aGFP) or *AtSUMO1* (WB a*AtS1*) antibodies. The migration of GFP:RGA and SUMOylated forms (*AtS1*-GFP:RGA) of GFP:RGA protein is indicated.

(D) Accumulation of GFP:RGA protein in 8 days old seedlings. Proteins derived from *pRGA::GFP:RGA ots1 ots2* and *pRGA::GFP:RGA OTS1 OTS2* lines originating from outcrossing the *pRGA::GFP:RGA* transgenic line (*Ler* background) with *ots1 ots2* (Col-0). Proteins are loaded in duplicated lanes, and Coomassie Blue filter staining (C. Blue) serves as a loading control.

(E) Accumulation of GFP:RGA protein in 8 days old *pRGA::GFP:RGA* seedlings in the wild-type (*OTS1 OTS2*) or mutants (*ots1 ots2*) backgrounds transferred to liquid cultures containing Cyclohexamide (CHX, 100 μM), (+), or mock control (DMSO), (-), for 1 hour. Coomassie Blue filter staining (C. Blue) serves as a loading control.

(F) GST:GAI SUMOylation in *E.coli* by activating (E1), conjugating (E2) enzymes and active (His:*AtS1*^{GG}) and inactive (His:*AtS1*^{AA}) *AtSUMO1*. A GST pull down of total *E. coli* extracts (input) is shown. Numbers indicate molecular mass (kDa), and the SUMOylated forms of GST:GAI are shown on the right. Asterisk indicates the

predominant SUMOylated band of GAI detected with GAI (left) and AtSUMO1 (right) antibodies. The extra bands revealed by AtSUMO1 antibodies likely derive from the non specific proteolysis of GST:GAI or other SUMOylated forms of GST:GAI.

Supplementary Figure 3. SUMOylation affects DELLA activity *in vivo*.

(A) Mean rosette size (maximum diameter) of 24 days old wild-type (*Ler wt*), *gal-5* and transgenic (T2) plants grown in soil under long days conditions. n= 16-18, Error bar = SEM.

(B) Image of 6 weeks old wild-type (*Ler wt*), *gal-5* and *35S::4Xmyc:OTS2 gal-5 #3* transgenic (T2) plants. Inset shows *gal-5* and *35S::4Xmyc:OTS2* plants one week later. Note the increased stem length and presence of open flowers and developing siliques in the transgenic line but not in the *gal-5* mutant. Scale 1cm.

(C) Main inflorescence length of wild-type (*Ler wt*), *gal-5* and transgenic (T2) plants *35S::4Xmyc:OTS2 gal-5* grown in soil conditions. Shown are mean values at the indicated time points after plate-grown seedlings (approximately 8 days old) were transferred to soil. Error Bar = SEM, n = 11-18 for each genotype.

(D) Flowering time (left) and plant height (right) phenotypic classes of T1 transgenic plants (*gal-5* background) transformed with empty vector (Vector), *35S::RGA:GFP*, or *35S::RGA^{K65R}:GFP*. The primary inflorescences of independent Basta resistant plants were measured after 8 weeks of growth in soil under long days.

(E) Image of representative T3 or T4 transgenic plants (*gal-5* background) transformed with empty vector (Vector), or *35S::RGA^{K65R}:GFP* *35S::RGA:GFP*. Pictures were taken after seven weeks of growth in soil under LDs conditions.

(F) Real-time PCR analysis of *RGA* transcripts levels in selected transgenic lines. Total RNA derived from 9 days old seedlings grown in petri dishes. Bars indicate the expression levels as fold change variations relatively to line *35S::RGA^{K65R}:GFP* #13 (which was arbitrarily set as 1). *ACTIN* was used for normalisation, error bars = SD of two technical replicates. Middle panel, accumulation of RGA:GFP or rga^{K65R}:GFP proteins in selected lines with similar transgene-derived expression levels. Blue filter staining (C. Blue) serves as a loading control. Western Blot is conducted with GFP antibodies. Lower panel, accumulation of RGA:GFP (line #2) or rga^{K65R}:GFP (line #7)

proteins in 8 days transgenic seedlings (*gal-5*). Seedlings were transferred to liquid cultures containing Cycloheximide (CHX, 100 μ M), (+) or mock control (DMSO), (-) for 3 hour. Coomassie Blue filter staining (C. Blue) serves as a loading control.

(G) Image of five-week-old plants grown under long day photoperiods. Hemizygous transgenic plants derive from a cross of *35S::RGA^{K65R}:GFP* (#2) and *35S::RGA:GFP* (#7) to wild-type (*Ler*).

(H) Mean rosette leaves number (RNL) in long day-grown plants scored after bolting.

Supplementary Figure 4. GID1a has a functional SIM motif in the N-terminal region.

(A) GST pull down assay between His:*AtSUMO1* and GST:*GID1a* or GST in the presence (+) or absence (-) of GA₃ (10 μ M). Asterisk indicates a cross-reacting band. Input and pulled-down proteins were probed with *AtSUMO1* (WB a*AtS1*) or GST (WB aGST) antibodies.

(B) Accumulation of *GID1a:TAP* proteins derived from independent T3 transgenic *35S::GID1a:TAP* young seedlings. Number indicates molecular mass (kDa). Non-transgenic, wild- type extracts (wt) were used as a negative control and Coomassie Blue filter staining (C. Blue) serves as a loading control.

(C) Mean root growth of 10 days old seedlings in the presence of 100 mM NaCl expressed as a percentage (%) relatively to the untreated controls. Error bar = SEM. n = 16 for each genotype / treatment combination.

(D) Mean root growth of 8 days old seedlings in the presence of 100 mM NaCl. The two experiments were run in parallel. Error bar = SEM. n = 32 for each genotype / treatment combination.

TABLES

List of primers used in this study

Oligo	Sequence (5'-3')	Amplicon
LC15	TTAATCTGTTTGGTTACCCTTGCGG	OTS2
LC18	GACAGGGATGCATATTTTGTGAAG	OTS2
LC69	CCGTCGGAGCTTTATTCTTG	RGA
LC70	TCGTTCCCTATGACTCCACCA	RGA
LC71	cgaaatggctgatgttgctcagagactcgagcagct	GAI
LC72	agctgctcgagtctctgagcaacatcagccattcg	GAI
LC73	CACCATGGCTGCGAGCGATGAAGT	GID1a
LC74	ACATTCCGCGTTTACAAACGC	GID1a
LC75	CACCCTAGATCCAAGATCAGACC	RGA
LC76	GTACGCCGCCGTCGAGAGT	RGA
LC77	GAGATGGCGGAGGTTGCTTTGAGACTCGAACAATTAG	RGA
LC78	CTAATTGTTTCGAGTCTCAAAGCAACCTCCGCCATCTC	RGA
LC80	CACCATGAAGAGAGATCATCATC	GAI
LC81	ATTGGTGGAGAGTTTCCAAG	GAI
LC85	GCCTCAAAGACACCTCTGG	OTS2
LC86	GCTTATCCAGCTTCCACGTC	OTS2
lcm26	CCGTCGGAGCTTTATTCTTGG	RGA
lcm27	CGTCGTTCCCTATGACTCCACC	RGA
lcm28	GCAAACCTAGATCCGACATTG	GAI
lcm29	GCTCCGCCGATTATAGTG	GAI
mr37	CTCTCCCGCTATGTATGTCGCCA	ACT2
mr38	GTGAGACACACCATCACCAG	ACT2

1

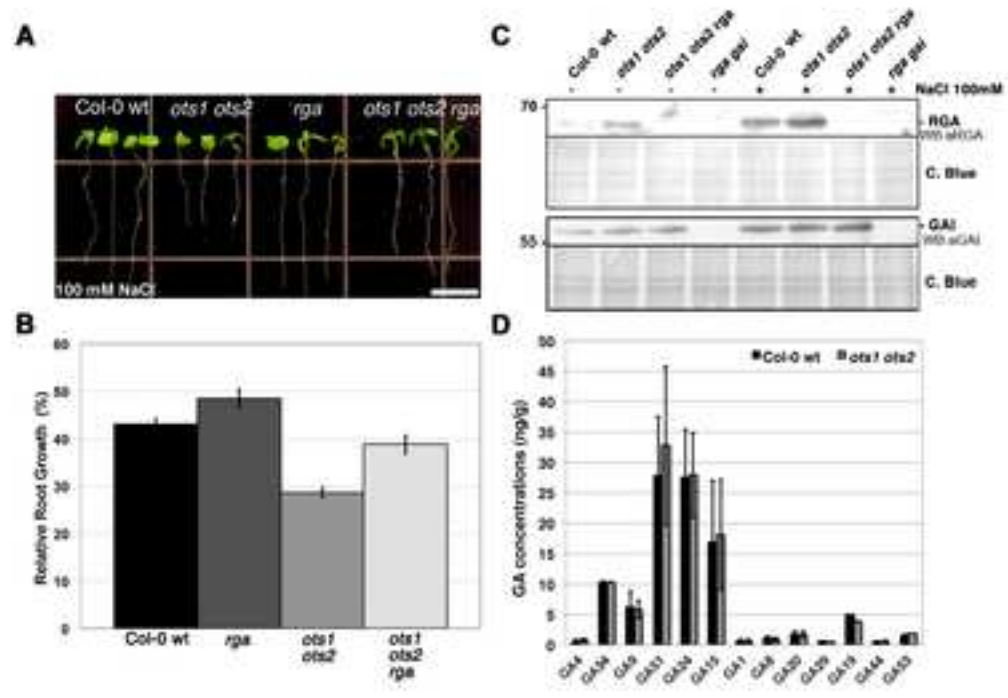


Figure 1

Figure 3
[Click here to download high resolution image](#)

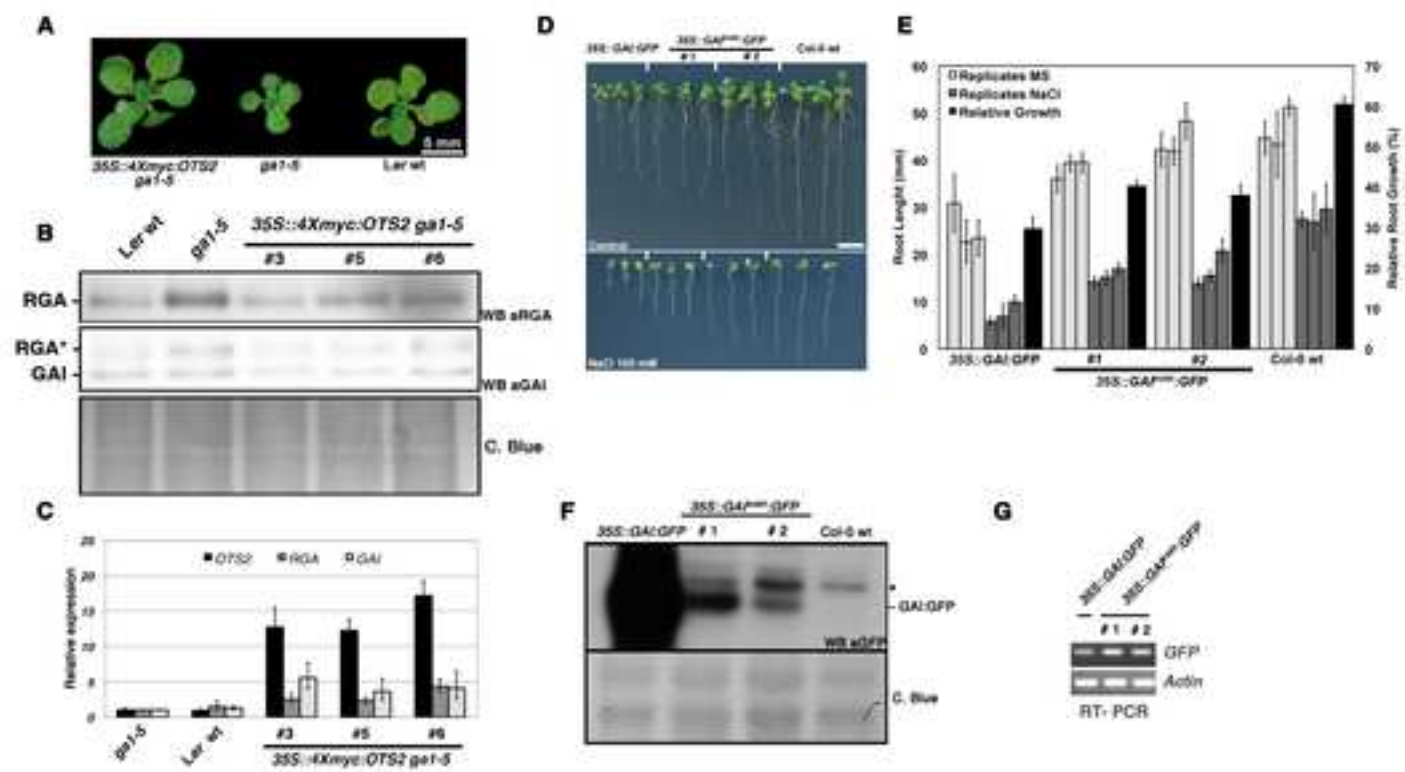


Figure 3

Figure 4
[Click here to download high resolution image](#)

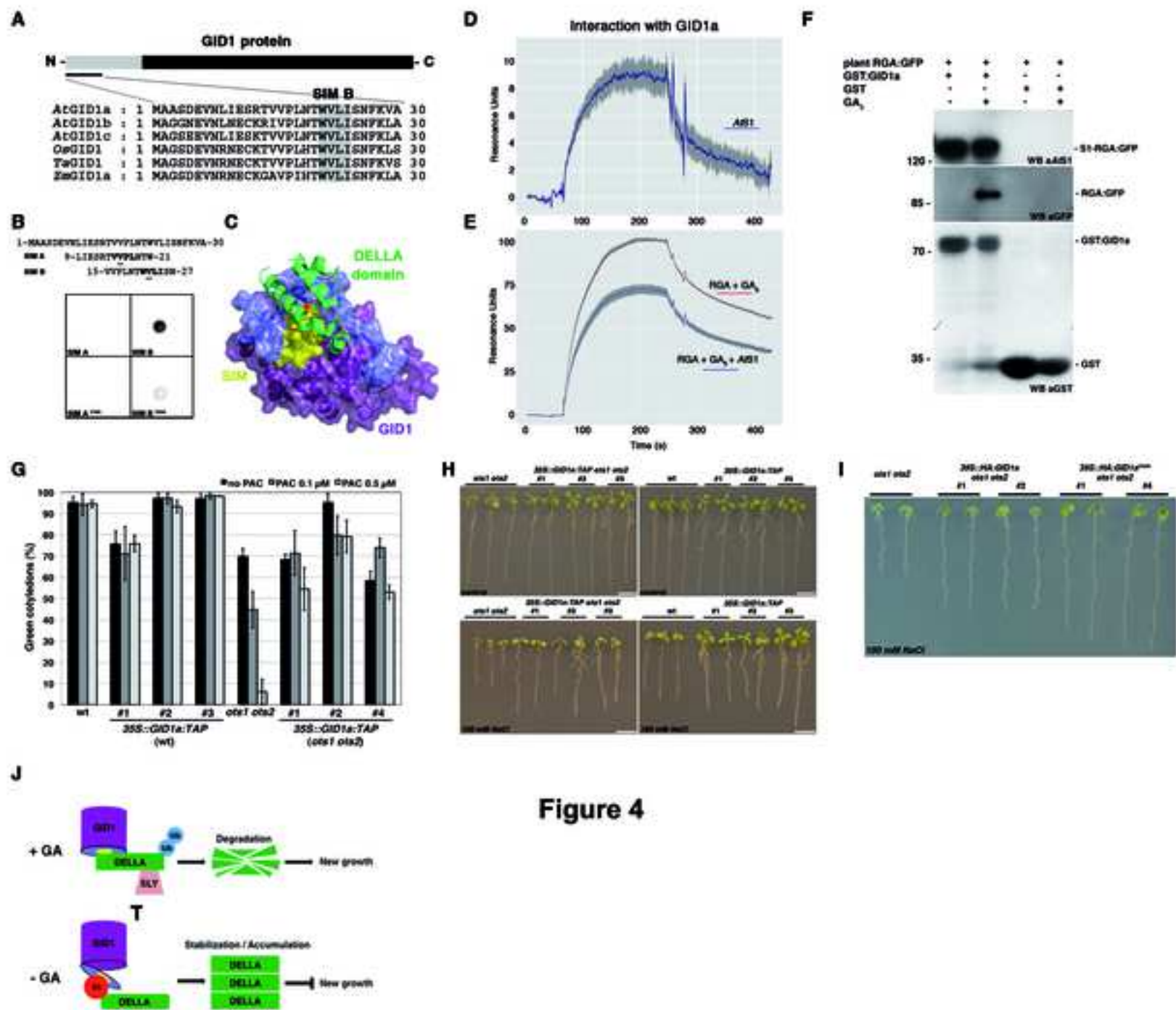


Figure 4

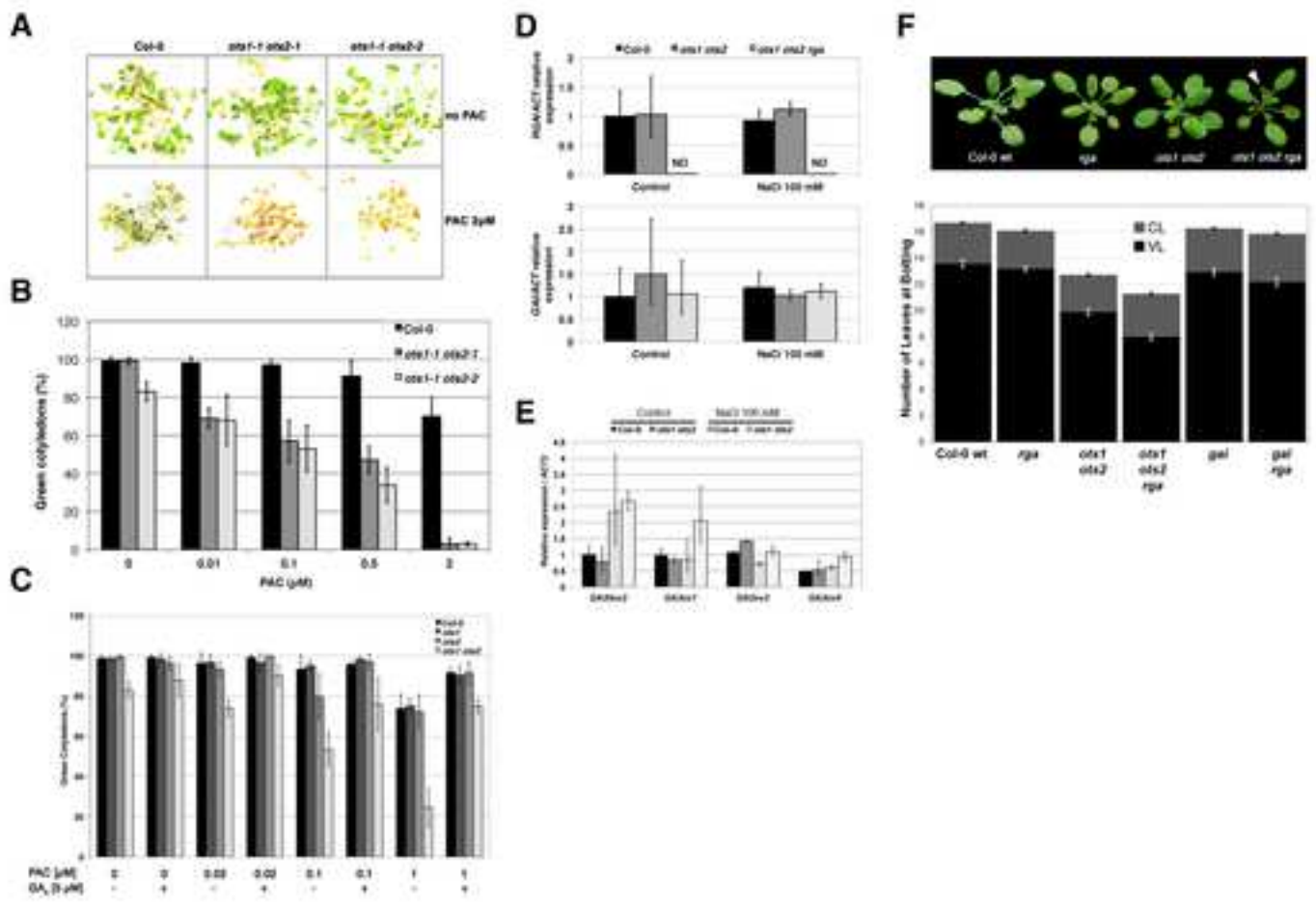


Figure S1

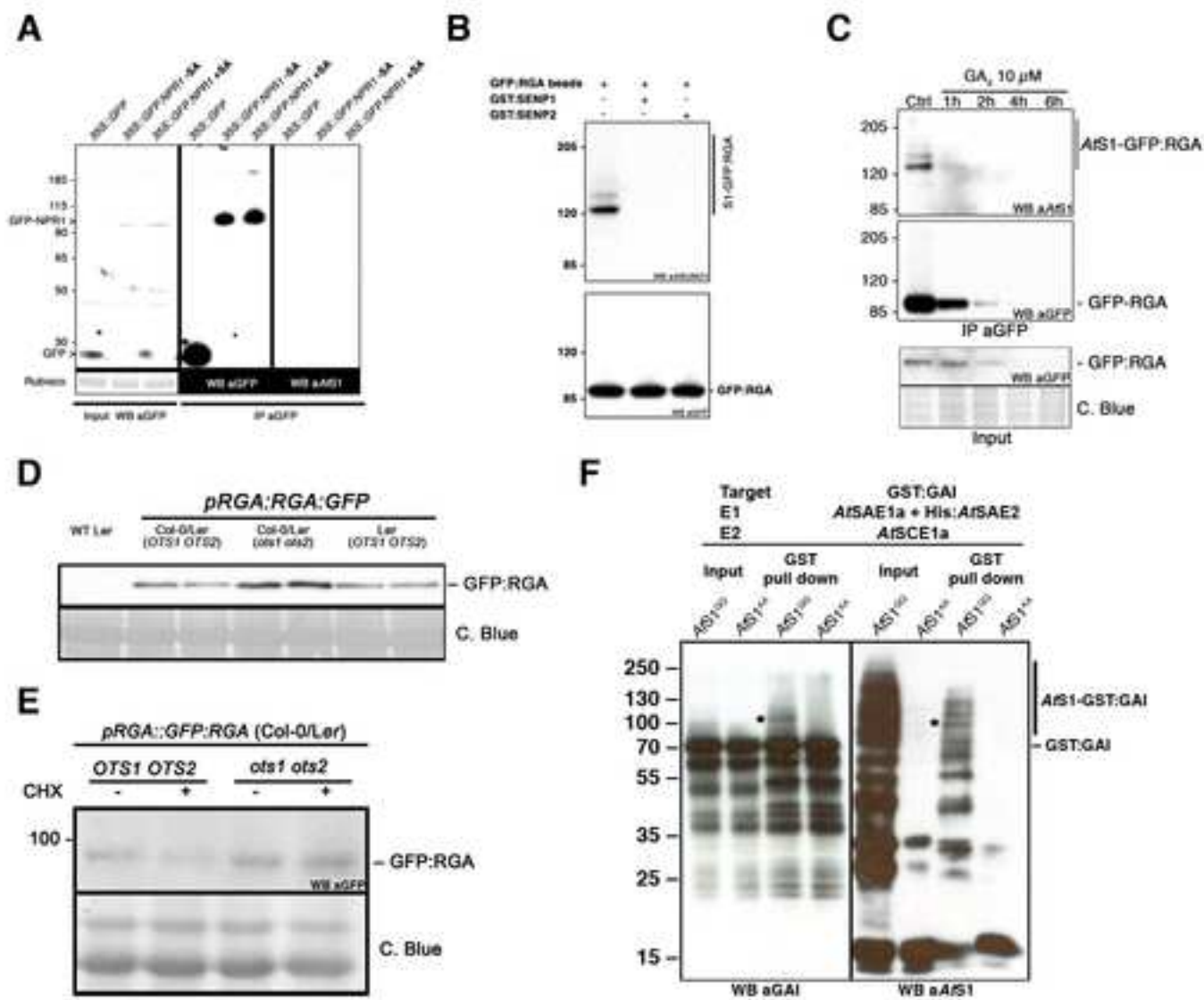


Figure S2

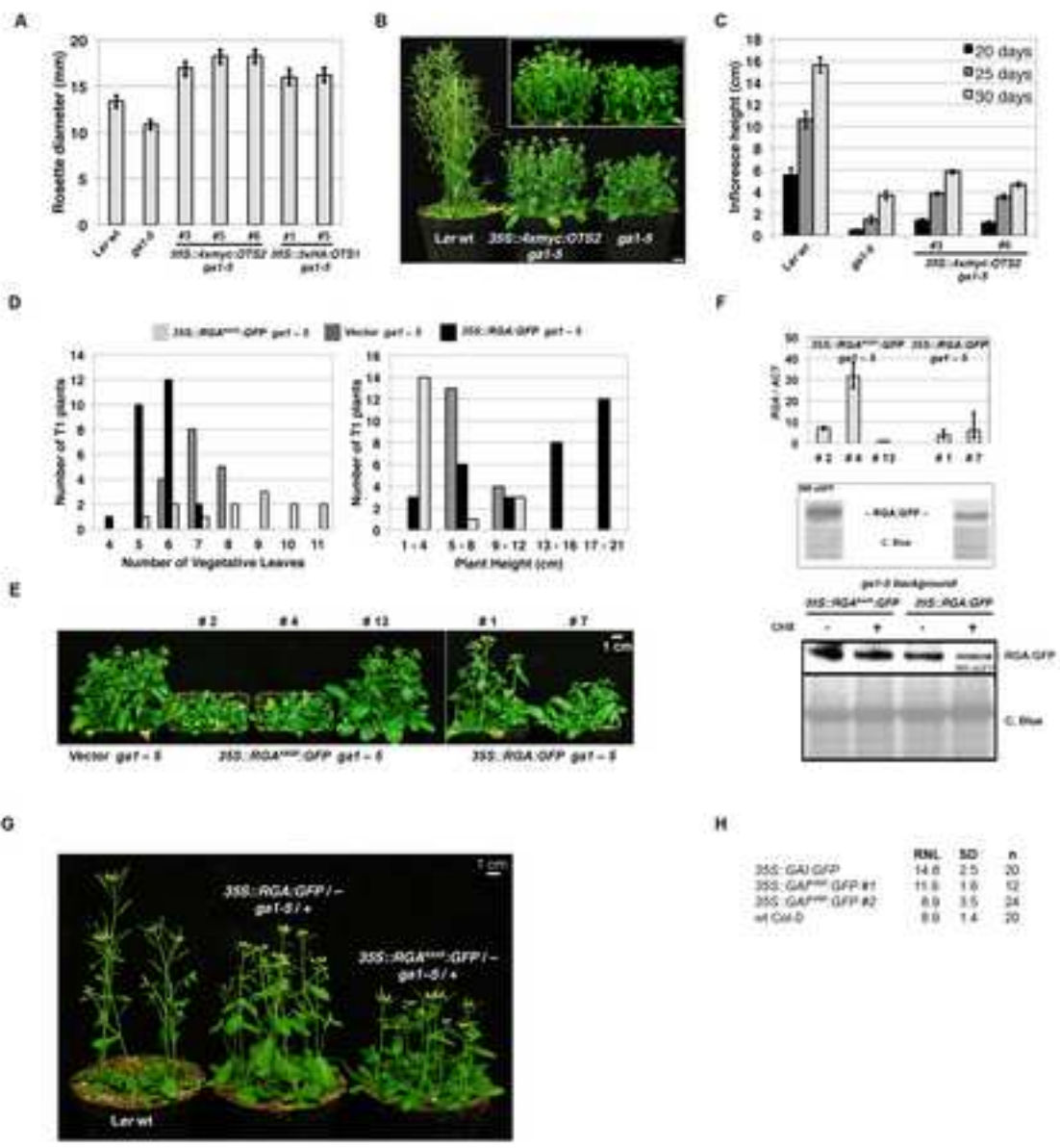


Figure S3

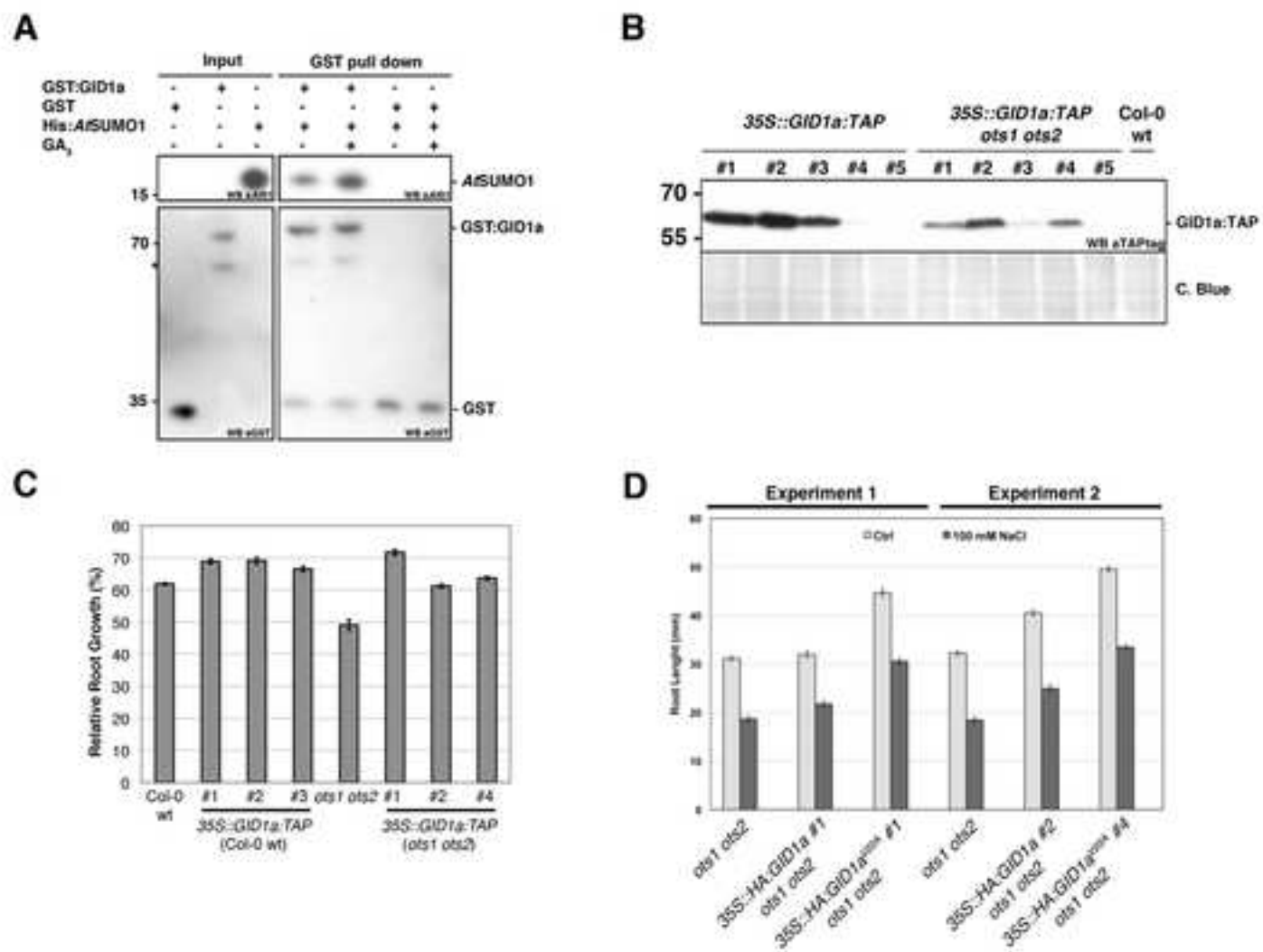


Figure S4